

## Temperature-induced particle self-assembly

Philip Born, Eoin Murray, Tobias Kraus\*

INM – Leibniz Institute for New Materials, Campus D2 2, 66123 Saarbücken, Germany

### ARTICLE INFO

#### Article history:

Received 2 June 2009

Accepted 18 September 2009

#### Keywords:

- A. Nanostructures
- C. Electron microscopy
- D. Phase transitions
- D. Superlattices

### ABSTRACT

Agglomeration of monodisperse thiol-stabilized gold particles with diameters of 6 nm, suspended in organic solvents, was induced by the cooling of the suspension. A sharp transition between the stable suspension and agglomeration resulted. The temperature of the transition depends on the concentration and the compatibility of the solvent. The morphology of the formed particle structures upon agglomeration implies that the used metal colloid can be described as a van der Waals-gas. The particles undergo phase transitions from a stable fluid phase to a metastable phase, in which nucleation and growth occur, or to an instable phase, in which spinodal decomposition occurs. The results will direct research on routes to nanostructured materials using nanoparticles as building blocks.

© 2009 Elsevier Ltd. All rights reserved.

### 1. Introduction

Many technologies, including optoelectronics, thermoelectrics, separation methods, functional coatings, and energetic materials, could profit from the ability to control the structure of materials on a nanometer length scale. One approach to synthesize nanostructured materials is to use suspended nanoparticles as building blocks [1–11]. Energetic materials will benefit from the higher reactivity due to the high surface-to-volume ratio and the lower ignition temperatures caused by the lower melting point [12]. A way to further improve a nanostructured energetic material is to control the arrangement of the particles in the system. When replacing a randomly close-packed granulate by a cubic close-packed system, the volume fraction occupied by particles increases from a maximum of 64% in the random system to 74% in the cubic system, thus increasing the stored chemical energy per unit volume. Additionally, the number of next neighbors for each particle doubles from 6 to 12 and the interparticle space is uniform, ensuring homogeneous combustion. Recent experiments have demonstrated that mixed nanoparticles can also form regular superstructures, in which the stoichiometry of the formed assemblies and the chemical environment of each individual particle are precisely controlled [8,9,11].

In many cases, the disorder–order transition for sub-micron particle suspensions can be described as a Kirkwood–Alder transition. When the particle volume fraction of the suspension exceeds 50%, there is a transition to an ordered state, in which the available volume per particle is maximized [13]. This transition is

purely an entropic effect and is dominant for particles with little van der Waals interaction such as polymer or oxide particles in water which can be treated as hard spheres. For metallic nanoparticles, however, agglomeration and ordering is observed at much lower volume fractions than required for a Kirkwood–Alder transition. The agglomeration of the particles to densely packed structures can be explained by the destabilization of the particles by shielding of the electrostatic repulsion [14,15] or adding incompatible solvents to suppress steric stabilization [1], or effects inside drying thin films or droplets of suspensions [16,17]. However, the process parameters which distinguish between randomly and cubic close-packing have yet to be elucidated.

Here we study the arrangement process of gold nanoparticles which directly assemble into superstructures from the bulk suspension. This experimental system excludes non-equilibrium processes and instabilities such as convective flow and confinement, effects that would complicate the description of the processes and hinder the search for basic concepts of particle arrangement. Varying the growth speed should clarify whether order is always achieved in equilibrium or if kinetic effects dominate, i.e. the particles get jammed under certain conditions before reaching the ordered state.

### 2. Experimental

#### 2.1. Nanoparticle synthesis

Low polydispersity is crucial to gain ordered close-packed structures of particles [18]. A synthetic route adapted from Zheng et al. [19] was used in this work. Gold nanoparticles were formed by a one-pot reduction of a gold source by an amine–borane

\* Corresponding author.

E-mail address: [tobias.kraus@inm-gmbh.de](mailto:tobias.kraus@inm-gmbh.de) (T. Kraus).

complex in the presence of an alkyl thiol. In a typical synthesis, 0.31 g chlorotriphenylphosphine gold (AuPPh<sub>3</sub>Cl, ABCR 98%) was stirred in 50 ml benzene (Riedel-de-Hahn >99.5%) forming a colorless solution. A mixture of 0.53 g tert-butylamineborane (Fluka 97%) and 0.18 ml dodecanethiol (Fluka >98%) was added to the AuPPh<sub>3</sub>Cl solution and reacted at 55 °C for 2 h. Following completion of the reduction reaction the deep red solution was cooled to room temperature, precipitated by the addition of ethanol and washed by centrifugation and subsequent resuspension in toluene. Finally, the particles were resuspended in heptane.

## 2.2. Characterization techniques

Transmission electron microscopy (TEM) was performed using a Philips CM 200 TEM operating at 200 keV with a point-to-point resolution of 0.24 nm and a lattice resolution of 0.14 nm. For selective-area small-angle electron diffraction (SASAED), the camera length was set to 4.7 m. For particle characterization, copper TEM grids with carbon coating were dipped into the suspension and were dried in an oven at 105 °C. To determine the mean size and size distribution of the gold cores of the particles, several hundred particles were evaluated.

In order to characterize particle structures grown in suspension at certain temperatures drying at elevated temperatures must be avoided. Therefore, TEM grids were dipped into the suspension with the particle agglomerates and then immediately into liquid nitrogen to vitrify them, and were finally freeze-dried in a vacuum of 10<sup>-5</sup> bar.

Dynamic light scattering (DLS) analysis was performed using a Wyatt Technology DynaPro Titan operating at a wavelength of 831.2 nm to measure the hydrodynamic radius of the particles. The thickness of the capping layer was calculated by subtracting the core radius measured with TEM from the hydrodynamic radius. The temperature in the sample chamber was varied between -8 and 60 °C with humidity control to avoid condensation of vapor.

The gold concentration was measured by inductively coupled plasma atomic emission spectroscopy (ICP-AES) on a Horiba Jobin Yvon Ultima 2 instrument. Results from diluted suspensions of the gold colloid were compared to a standard gold salt solutions concentration curve for quantitative analysis.

## 2.3. Growth experiments

The growth of particle assemblies in bulk liquids was monitored *in-situ* by DLS. The sample temperature was decreased in steps of 1 K and equilibrated for 1 min, followed by a DLS measurement of 100 s. When the cumulant fit of the autocorrelation function showed an increase in the mean particle diameter, the sample was heated again above the threshold temperature to disassemble the particle structures. By setting and maintaining a temperature close to or far below the threshold temperature, the agglomeration rate could be adjusted.

## 3. Results

### 3.1. Particle characterization

In Fig. 1 a typical TEM image of the gold particles synthesized with dodecanethiol as a stabilizer can be seen. The particles form hexagonally close-packed layers; the particle distance is determined by the minimum of the interparticle potential. A good size and shape uniformity is visible. An overview of

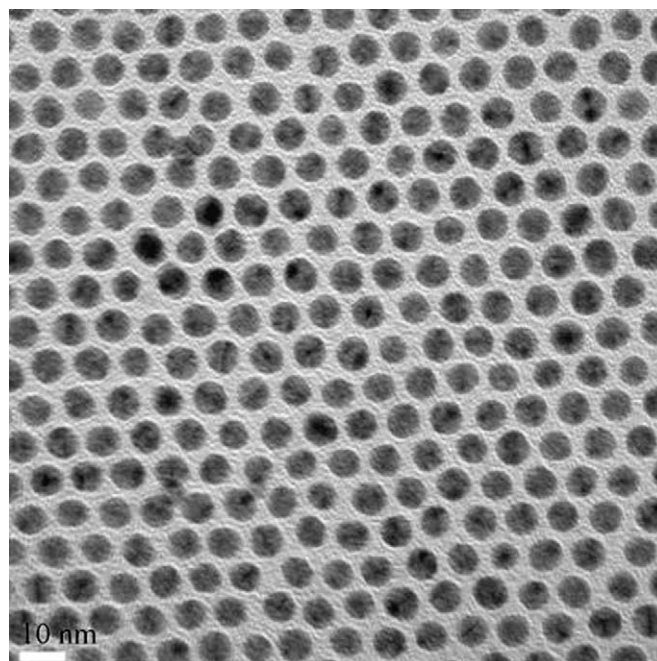


Fig. 1. Transmission electron micrograph of dodecanethiol-capped gold particles. The scale bar corresponds to 10 nm.

Table 1  
Overview over particle characterization results.

capping ligand	$r_c$ (nm)	$r_H$ (nm)	$l_{CL}$ (nm)	Conc. (parts per ml <sup>-1</sup> )
C <sub>10</sub> -thiol	2.9 (17%)	4.2 (12%)	1.3	
C <sub>12</sub> -thiol	2.8 (10%)	4.5 (10%)	1.7	$2.74 \times 10^{15}$
C <sub>16</sub> -thiol	2.1 (19%)	5.0 (24%)	2.9	$1.62 \times 10^{14}$
C <sub>18</sub> -thiol	2.7 (18%)	5.8 (9%)	3.1	

$r_c$  is the radius of the gold core measured with TEM,  $r_H$  the hydrodynamic radius measured with DLS,  $l_{CL}$  the thickness of the capping layer, and Conc. the concentration measured with ICP-AES. Polydispersities are given in brackets.

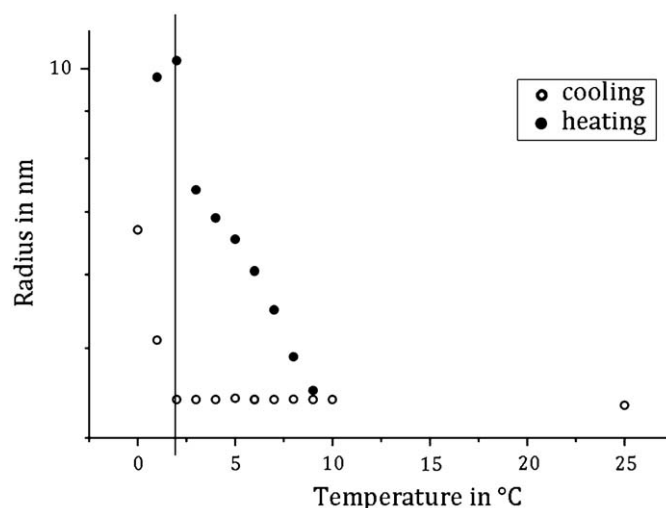
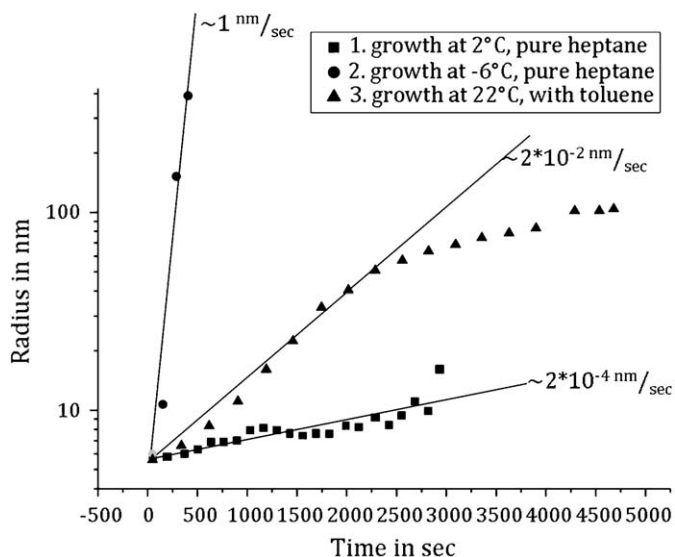


Fig. 2. Typical DLS measurement of a temperature-induced particle agglomeration. Below 3 °C the particles agglomerate, above 3 °C the agglomerates disassemble again.

particle characterization results is given in Table 1. Notable is the minimum in polydispersity for the sample synthesized with dodecanethiol, which was used for further experiments.

n-Heptane was found to be the best solvent in terms of particle stability. In solvents with even only slightly higher polarity, such as chloroform or toluene, DLS confirmed that small particle agglomerates were always present at room temperature.



**Fig. 3.** Hydrodynamic radius as function of time measured with DLS at different temperatures. Noteworthy is the high agglomeration rate at  $-6^{\circ}\text{C}$ .

### 3.2. Growth of particle superlattices

A dependence of the particle stability on temperature was observed. Cooling the suspension eventually led to agglomeration of the particles, indicated by an increase of the hydrodynamic radius measured by DLS. A typical temperature-induced transition between a stable gold colloid and particle agglomeration can be seen in Fig. 2. When this sample is cooled below  $3^{\circ}\text{C}$ , agglomeration begins. The agglomeration ceases only when the temperature is increased above the threshold. The agglomerates disassemble and the hydrodynamic radius returns to the value of free particles. Using known transition temperatures, variable growth rate experiments can be performed and the influence of the growth rate on the particle ordering can be observed. One might assume that a fast growth would lead to a jamming of the particles and prevent ordering.

By setting the temperature just below the transition threshold, slow growth ( $10^{-4}\text{ nm s}^{-1}$  at  $2^{\circ}\text{C}$ ) of the particle agglomerates was observed (Fig. 3). By cooling further, a faster agglomeration ( $1\text{ nm s}^{-1}$  at  $-6^{\circ}\text{C}$ ) was induced. The agglomerates grown at a low growth rate had diameters of roughly  $100\text{ nm}$  and showed no order as shown in Fig. 4. The structures grown at the lower temperature formed large percolating networks, again with no ordering of particles.

To test the influence of the absolute temperature, the transition temperature was altered. The transition temperature depends on the concentration of the suspension. A test series of transition measurements at different concentrations is given in Fig. 5. Another way to increase the transition temperature is to add a

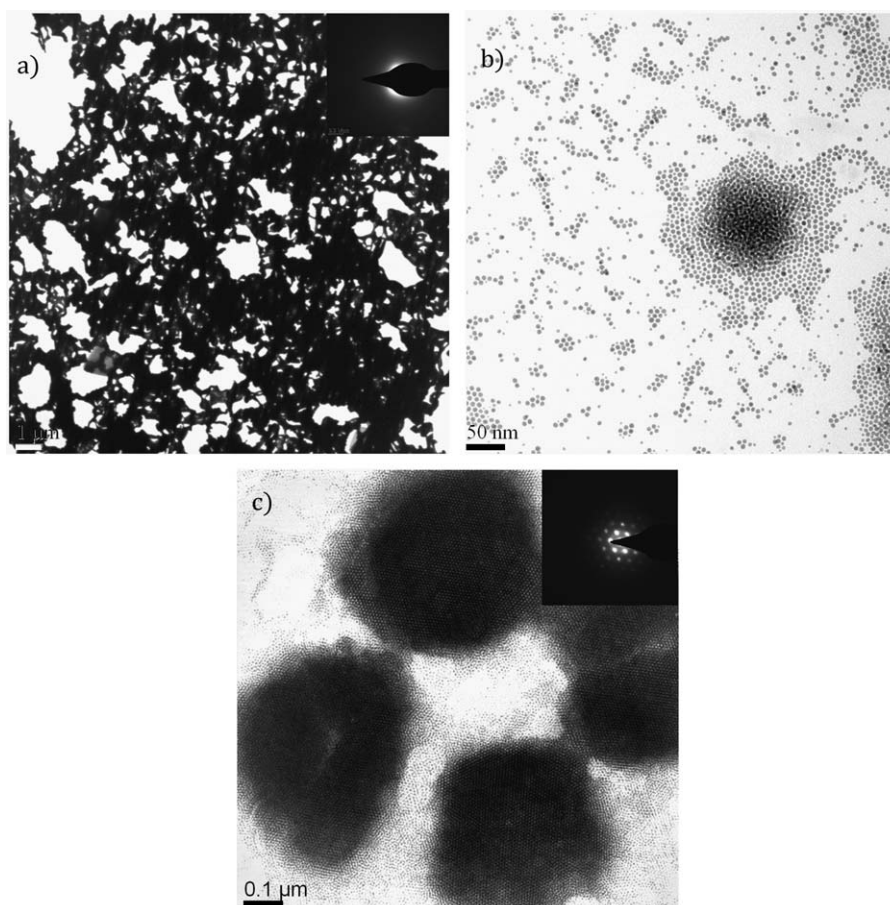


**Fig. 4.** Particle agglomerates grown at (a)  $-6^{\circ}\text{C}$ , (b)  $2^{\circ}\text{C}$ , and (c)  $22^{\circ}\text{C}$ . The insets show SAED patterns, proving the ordering of the agglomerates grown at  $22^{\circ}\text{C}$ . Scale bars correspond to (a)  $1\text{ }\mu\text{m}$ , (b)  $50\text{ nm}$ , and (c)  $0.1\text{ }\mu\text{m}$ .

slightly more polar solvent to the suspension. With 10% toluene in the suspension, the transition temperature has shifted above room temperature and allows an intermediate growth rate of  $10^{-2} \text{ nm s}^{-1}$  at  $22^\circ\text{C}$  (Fig. 3). The agglomerates grown at this temperature had excellent particle ordering (Fig. 4), although the growth rate was much higher than for the structures grown at  $2^\circ\text{C}$ . These results suggest that the absolute temperature, not the growth rate, is responsible for the close-packing of the particles.

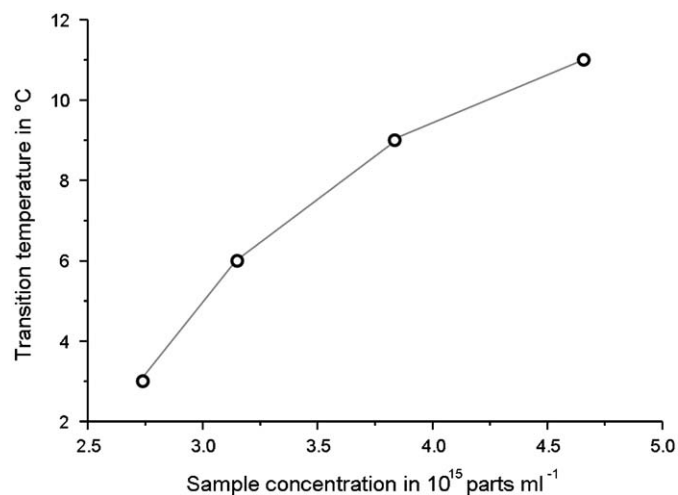


Fig. 5. The transition temperature as function of the sample concentration, as measured with DLS. The lines are guidelines for the eye.

Dipping of the TEM grid creates a thin liquid film that may have an influence on the particle agglomerates. To rule this effect out, test tubes containing a TEM grid were filled with  $100 \mu\text{m}$  of gold suspension using pure heptane as solvent and were placed in a small temperature-controlled and convection-free chamber to allow solvent evaporation. Evaporation of the liquid in the small chamber took approximately a day at room temperature and up to several days at lower temperature. Thus the drying occurred on time scales far removed from the particle time scales for diffusion and relaxation. The results (Fig. 6) correlate well with the structures grown earlier. At  $-20^\circ\text{C}$ , large percolating agglomerates of unordered particles remain on the grid. At  $5^\circ\text{C}$ , ordered micrometer-sized agglomerates and unordered agglomerates with a diameter of several hundred nanometers are formed. At  $20^\circ\text{C}$ , well ordered agglomerates with diameters of several hundred nanometers are deposited, which probably formed in the later stages of the evaporation when the loss of solvent had increased the concentration and transition temperatures near room temperature were attained.

#### 4. Discussion

We found that a suspension of sterically stabilized metallic nanoparticles undergoes a transition from a stable dispersed state to an unstable state when it is cooled. The temperature at which the transition occurs depends on the concentration of the suspension. The condensates formed in the unstable state can be either small, almost spherical agglomerates, or (at lower temperatures) large percolating networks resembling structures

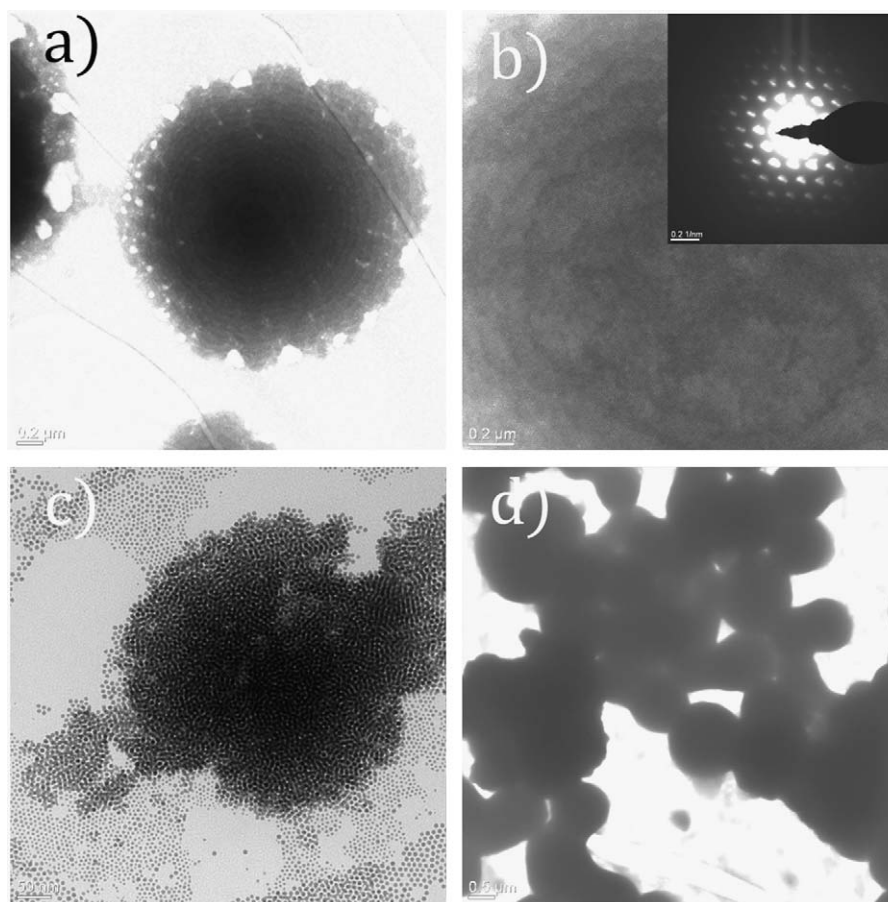


Fig. 6. Particle structures grown at (a)  $20^\circ\text{C}$ , (b) and (c)  $5^\circ\text{C}$ , and (d)  $-20^\circ\text{C}$ . (b) and (c) show the coexistence of ordered and unordered agglomerates. The scale bars correspond to (a)  $0.2 \mu\text{m}$ , (b)  $0.2 \mu\text{m}$ , (c)  $50 \text{ nm}$ , and (d)  $0.5 \mu\text{m}$ . Inset in (b) shows the SASASED pattern of the agglomerate.

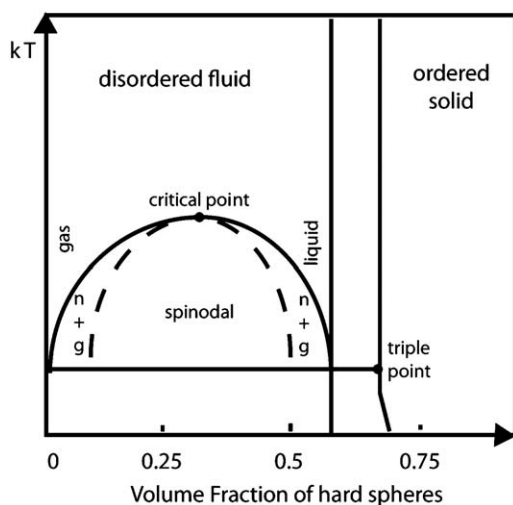


Fig. 7. Schematic phase diagram of a hard sphere system interacting via a Lennard–Jones potential (adapted from [21]).

formed by spinodal decomposition. Ordering only occurs for particle assembly at high temperatures, despite of the slow assembly process at low temperatures.

According to the model of Edwards and Dolan [20], the interparticle potential of two sterically stabilized particles can be described by the formula

$$V = -\frac{16}{9} \frac{r^6}{d^6} A_{Ham} + \frac{Nk_b T}{A} 2e^{-(3d^2/2l)},$$

where  $r$  is the particle radius,  $d$  the surface separation of the particles,  $A_{Ham}$  the Hamaker-coefficient,  $N$  the number of interacting polymers,  $A$  the interacting surface,  $k_b T$  the thermal energy,  $l$  the linker length, and  $L$  the length of the ligand.

This interaction potential consists of an attractive van der Waals-potential and a steep repulsive potential that is due to the steric interaction of the ligand shells of the particles. It resembles the Lennard–Jones potential; an analogy that we exploit for the interpretation of our results. Fig. 7 shows a schematic phase diagram for spheres interacting via a Lennard–Jones potential [21]. Characteristic features are the Kirkwood–Alder transition from fluid to solid at 50% of the volume occupied by the spheres, the existence of a critical temperature below which a fluid–fluid phase transition from gas to liquid occurs, and the separation of the phases either by binodal or spinodal decomposition. Our suspensions had a low nanoparticle volume fraction occupied by gold particles, close to 0.05%, far left of the critical temperature in the phase diagram.

Interpreting the gold particles in the suspension as molecules of a van der Waals-gas can qualitatively explain our observations. Cooling the suspension will lead to a metastable regime, where a phase separation occurs by nucleation and growth (i.e. by binodal decomposition). Cooling further leads to the unstable regime, where spinodal decomposition takes place and results in the observed large particle networks. Increasing the concentration shifts the decompositions to higher transition temperatures.

Quantitative predictions require knowledge of the exact shape of the interparticle potential. There has been extensive study to theoretically determine the phase diagram for particles interacting via different potentials (a review is given in [22]). Importantly, Zaccarelli et al. [23] have shown that with decreasing range of the attractive part of the potential, the critical temperature and the

fluid–fluid transition disappear. Thus the shape of the particle potential determines whether the phase separation leads to an ordered solid phase or an unordered liquid phase of the particles.

Treating the suspension as a van der Waals-gas quite accurately accounts for the agglomeration behavior, but it does not fully explain the temperature-dependence of the ordering. To describe this behavior, it may be necessary to take into account parameters such as particle kinetic energy or particle mobility. Consequently it may be possible to assign regions in a phase diagram, where particles form ordered structures and to make predictions for other particle systems.

## 5. Conclusions

Agglomeration of gold nanoparticles has been studied as a function of the temperature. Phase behavior similar to that of a van der Waals-gas was observed, explaining the general conditions which are necessary for the formation of ordered particle superstructures. To obtain a well-aligned close-packed mesoscopic material, the binodal decomposition line of the source suspension must be determined. The temperature must then be adjusted to start nucleation and growth but still keeps the suspension from spinodal decomposition.

However, the process of structure formation is not yet fully understood and can probably not be described by a temperature–concentration phase diagram. Although quantitative predictions of the phase behavior for different systems cannot yet be made, the qualitative result should be transferrable to similar colloids with strong van der Waals interaction, e.g. metals such as aluminum or iron and other materials with interesting energetic applications.

## References

- [1] C.B. Murray, C.R. Kagan, M.G. Bawendi, *Annu. Rev. Mater. Sci.* 30 (2000) 510–545.
- [2] Y. Xia, B. Gates, Y. Yin, Y. Lu, *Adv. Mater.* 12 (2000) 693–713.
- [3] S.C. Glotzer, M.J. Solomon, *Nat. Mater.* 6 (2007) 557–562.
- [4] S.H. Park, Y. Xia, *Langmuir* 15 (1999) 266–273.
- [5] L. Malaquin, T. Kraus, H. Schmid, E. Delamarche, H. Wolf, *Langmuir* 23 (2007) 11513–11521.
- [6] J. Tien, A. Terfort, G. Whitesides, *Langmuir* 13 (1997) 5349–5355.
- [7] M. Giersig, P. Mulvaney, *Langmuir* 9 (1993) 3408–3413.
- [8] E.V. Shevchenko, D.V. Talapin, C.B. Murray, S. O'Brien, *J. Am. Chem. Soc.* 128 (2006) 3620–3637.
- [9] E.V. Shevchenko, D.V. Talapin, N.A. Kotov, S. O'Brien, C. Murray, *Nature* 439 (2006) 55–59.
- [10] T. Still, W. Cheng, M. Retsch, U. Jonas, G. Fytas, *Phys.: Condens. Matter* 20 (2008) 1–9.
- [11] M.E. Leunissen, C.G. Christova, A.-P. Hynninen, C.P. Royall, A.I. Campbell, A. Imhof, M. Dijkstra, R. van Roij, A. van Blaaderen, *Nature* 437 (2005) 235–240.
- [12] Y. Huang, G.A. Risha, V. Yang, R.A. Yetter, *Combust. Flame* 156 (2009) 5–13.
- [13] A.P. Gast, W.B. Russel, *Phys. Today* 51 (1998) 24–30.
- [14] A.O. Lundgren, F. Björefors, L.G.M. Olofsson, H. Elwing, *Nano Lett.* 8 (2008) 3989–3992.
- [15] M.Y. Lin, H.M. Lindsay, D.A. Weitz, R.C. Ball, R. Klein, P. Meakin, *Phys. Rev. A* 41 (1990) 2005–2020.
- [16] B.A. Korgel, S. Fullam, S. Connolly, D. Fitzmaurice, *J. Phys. Chem. B* 102 (1998) 8379–8388.
- [17] M.G. Constantinides, H.M. Jaeger, X. Li, J. Wang, X.-M. Lin, *Z. Kristallogr.* 222 (2007) 595–600.
- [18] S.E. Phan, W.B. Russel, J. Zhu, P.M. Chaikin, *J. Chem. Phys.* 108 (1998) 9789–9795.
- [19] N. Zheng, J. Fan, G.D. Stucky, *J. Am. Chem. Soc.* 128 (2006) 6550–6551.
- [20] A. Dolan, S. Edwards, *Proc. R. Soc. A* 337 (1974) 509–516.
- [21] R.A.L. Jones, in: *Soft Condensed Matter*, Oxford University Press, 2002, p. 67.
- [22] G. Malescio, *J. Phys., Condens. Matter* 19 (2007) 1–23.
- [23] E. Zaccarelli, F. Sciortino, P. Tartaglia, G. Foffi, G. McCullagh, A. Lawlor, K. Dawson, *Phys. A* 314 (2002) 539–547.